

## Oligomer-specific A $\beta$ toxicity in cell models is mediated by selective uptake

Sidhartha M. Chafekar<sup>a</sup>, Frank Baas<sup>b</sup>, Wiep Scheper<sup>a,b,\*</sup>

<sup>a</sup> Neurogenetics Laboratory Academic Medical Center, University of Amsterdam, 1105 AZ Amsterdam, The Netherlands

<sup>b</sup> Department of Neurology, Academic Medical Center, University of Amsterdam, 1105 AZ Amsterdam, The Netherlands

### ARTICLE INFO

#### Article history:

Received 26 February 2008

Received in revised form 3 June 2008

Accepted 3 June 2008

Available online 13 June 2008

#### Keywords:

Alzheimer's disease

$\beta$ -amyloid

Aggregation

Oligomer

Toxicity

Uptake

### ABSTRACT

Alzheimer's disease (AD) is characterized by the aggregation and subsequent deposition of misfolded  $\beta$ -amyloid (A $\beta$ ) peptide. Previous studies show that aggregated A $\beta$  is more toxic in oligomeric than in fibrillar form, and that each aggregation form activates specific molecular pathways in the cell. We hypothesize that these differences between oligomers and fibrils are related to their different accessibility to the intracellular space. To this end we used fluorescently labelled A $\beta_{1-42}$  and demonstrate that A $\beta_{1-42}$  oligomers readily enter both HeLa and differentiated SK NSH cells whereas fibrillar A $\beta_{1-42}$  is not internalized. Oligomeric A $\beta_{1-42}$  is internalized by an endocytic process and is transported to the lysosomes. Inhibition of uptake specifically inhibits oligomer but not fibril toxicity. Our study indicates that selective uptake of oligomers is a determinant of oligomer specific A $\beta$  toxicity.

© 2008 Elsevier B.V. All rights reserved.

### 1. Introduction

One of the most prominent neuropathological hallmarks in brains of Alzheimer's disease (AD) patients is the deposition of senile plaques, extracellular lesions primarily composed of  $\beta$ -amyloid (A $\beta$ ). A $\beta$  is a 40 or 42 amino acid peptide derived from the amyloid precursor protein (APP) by proteolytic processing. Genetic and neuropathological studies provide strong evidence for a central role of A $\beta$  in the pathogenesis of AD [1–3].

One of the main questions still under debate concerning A $\beta$  toxicity is the (sub-) cellular localization of action. A $\beta$  is secreted into the extracellular space and finally deposited in the amyloid plaques in AD brain. Moreover, A $\beta$  is toxic to various cell types in culture when applied extracellularly [4–6]. This provides strong evidence for A $\beta$  exerting its toxic action from the outside of the cell. In addition to the deposition of A $\beta$  peptides into extracellular plaques there is a large number of studies now providing evidence for the presence of A $\beta$  within neurons on post-mortem AD and transgenic mouse brains (as reviewed in [7,8]). A $\beta$  is produced intracellularly in a variety of subcellular compartments, including the endoplasmic reticulum (ER), the Golgi apparatus and lysosomes [9–12]. A triple transgenic AD mouse model (3xTg) was established that displays cognitive impairments before plaque formation [13]. Here, deficits in synaptic

plasticity, learning, and memory appear to be induced by the buildup of intraneuronal A $\beta$ . Anti-A $\beta$  immunization results in clearance of extracellular A $\beta$  before intracellular A $\beta$  in these mice. After removal of the antibody, the intraneuronal accumulation of A $\beta$  reappears before the extracellular A $\beta$  deposits [14], indicating a dynamic exchange between the intra- and extracellular A $\beta$  pools. These studies demonstrate the importance of intracellular A $\beta$  in the pathogenesis of AD, however, the respective contribution of extracellular and intracellular A $\beta$  in AD disease progression is still elusive. In addition, it is unknown whether intraneuronal A $\beta$  originates from retention and subsequent aggregation of intracellularly generated A $\beta$  or from reuptake of extracellular A $\beta$ .

Another major issue in the toxicity of A $\beta$  is the pathophysiological role of the different aggregation species of A $\beta$ . The A $\beta$  peptide can exist in diverse assembly states [15]. Apart from the monomeric state and the fibrillar end-stage, different intermediate species such as low molecular weight oligomers (like dimers and trimers), larger more globular oligomers (A $\beta$ -derived diffusible ligands) and proto-fibrils have been reported. *In vitro*, both oligomeric as well as fibrillar preparations of A $\beta$  induce cell death in virtually any cell type in culture, but oligomeric preparations do so more potently [16–18]. These different assembly forms thus greatly differ in their neurotoxic potential while also the molecular mechanisms they activate are shown to be specific for the aggregation state. For example, small oligomers are shown to cause an impairment of long term potentiation [19,20] and endoplasmic reticulum (ER) stress [21], whereas the neuroinflammatory response appears to involve more fibrillar A $\beta$  [22].

The current study addresses the mechanism underlying these aggregation-state specific effects. One possible explanation is a

\* Corresponding author: Academic Medical Center, Neurogenetics Laboratory, P.O. Box 22660, 1100 DD Amsterdam, The Netherlands. Tel.: +31 20 5664959; fax: +31 20 5669312.

E-mail address: [w.scheper@amc.uva.nl](mailto:w.scheper@amc.uva.nl) (W. Scheper).

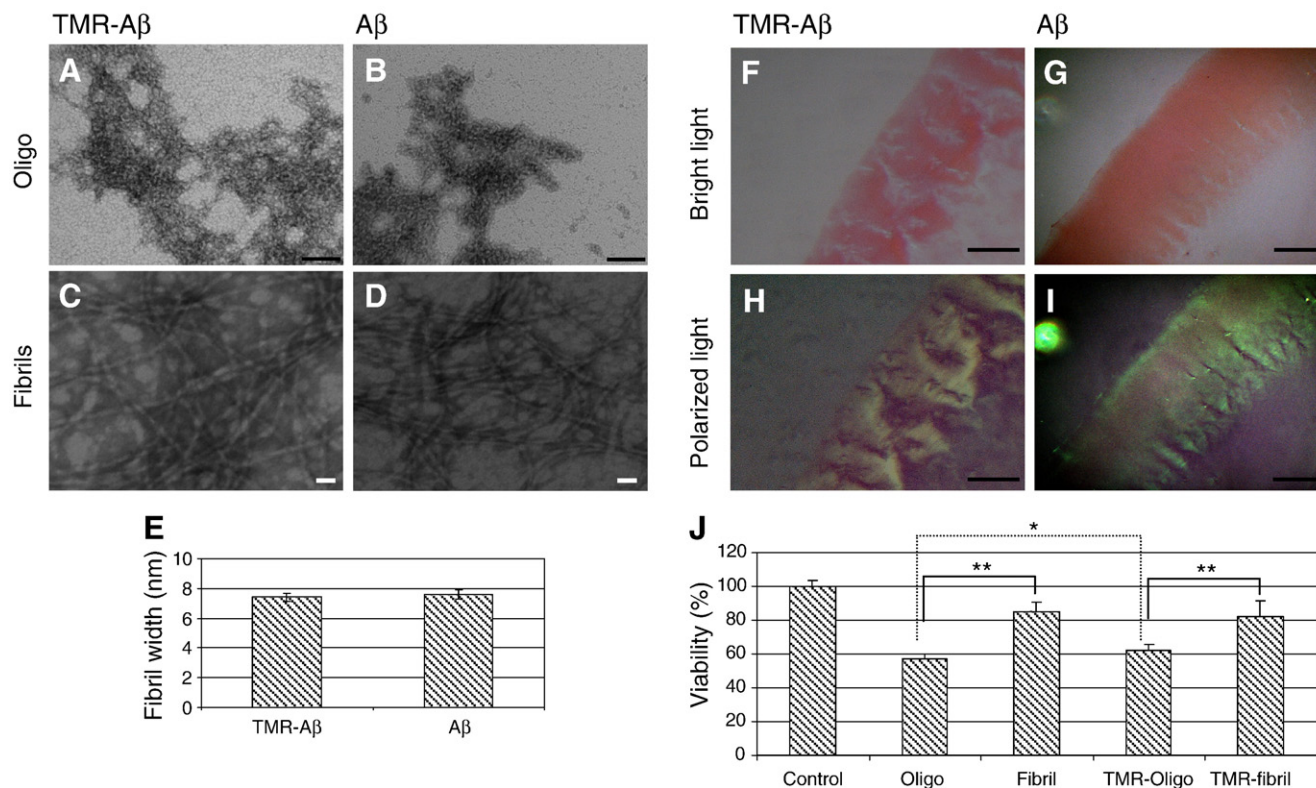


**Fig. 1.** Preparations enriched in oligomeric (Oligo) and fibrillar (Fibrils)  $A\beta_{1-42}$  were prepared as described in Materials and methods. Representative electron microscope images of oligomeric (A–B) and fibrillar (C–D) preparations of TMR-labelled  $A\beta_{1-42}$  and  $A\beta_{1-42}$  using negative stain. (Scale bar: 100 nm (A,B); 30 nm (C,D)). (E) The width of  $A\beta$  fibrils (in nm) on TEM was measured using the AnalySIS © software. Graph represents the mean  $\pm$  S.D. for  $n \geq 30$  from two separate experiments. (F–I) The  $\beta$ -sheet content of  $A\beta$  fibrils as well as TMR-labelled  $A\beta$  fibrils was analyzed using Congo Red (CR) staining, as described in Materials and methods. Shown are bright light pictures from TAMRA- $A\beta$  fibrils (F) and  $A\beta$  (G) stained with CR and polarized light pictures (H, I) to analyze the CR birefringence, indicative for their  $\beta$ -sheet content. (Scale bars: 100  $\mu$ m). (J) SK-N-SH cells differentiated for 5 days were treated in the absence (Control) or presence of 10  $\mu$ M oligomeric or fibrillar TMR- $A\beta_{1-42}$  or unlabelled  $A\beta_{1-42}$  for 48 h. Viability of the cells was determined by MTT assay and is depicted as percentage of control. The graph represents the mean  $\pm$  S.D. for  $n = 6$  from triplicate wells from two independent experiments. \* $p < 0.05$ ; \*\* $p < 0.001$  (Student's *t*-test).

differential accessibility of different aggregation states to the intracellular space of the cell. We show selective uptake of oligomers in different cell types. Preventing oligomeric  $A\beta$  from entering the cell reduces its toxicity whereas the toxicity of extracellular located fibrils is not affected. Our study thus indicates that selective uptake contributes to oligomer-specific toxicity.

## 2. Materials and methods

### 2.1. Antibodies and reagents

Cell culture reagents were purchased from Gibco BRL (Gaithersburg, MD, USA). Synthetic  $A\beta_{1-42}$  and TMR labelled  $A\beta_{1-42}$  peptide was purchased from Anaspec (San Jose, CA, USA). Vectashield was from Vector Laboratories (Burlingame, CA, USA). Rabbit anti Calnexin antibody was from Calbiochem (San Diego, CA, USA). Alexa-488 labelled Transferrin (Tfn) and LysoTracker Green was from Molecular Probes (Leiden, The Netherlands). All other chemicals were from Sigma (St Louis, MO, USA).

### 2.2. Cell culture

SK NSH human neuroblastoma cells and HeLa cells were maintained in DMEM supplemented with 10% foetal calf serum (FCS), 100 U/ml penicillin, 100  $\mu$ g/ml streptomycin and 300  $\mu$ g/ml glutamine. For use in experiments SK-N-SH human neuroblastoma cells were differentiated for 5 days using cell culture medium supplemented with 10  $\mu$ M Retinoic Acid.

### 2.3. Peptide solubilization and aggregation

$A\beta_{1-42}$  preparations enriched in oligomers and fibrils were obtained essentially as described in [21]. For the experiments conducted with TMR- $A\beta$ , unlabelled  $A\beta_{1-42}$  (in HFIP) was spiked with TMR-labelled  $A\beta_{1-42}$  (in HFIP) at a ratio of 1:2 (TMR- $A\beta$ : $A\beta$ ). This mixture was evaporated using a Speedvac and subsequently used for preparing TMR-oligomers and TMR-fibrils applying the same procedure as described above.  $A\beta$  treatments were performed in cell culture medium without phenol red.

### 2.4. Congo Red staining

$A\beta$  preparations were spotted on a cover slip as a 5  $\mu$ l droplet and left to dry. The dried specimen was subsequently fixed with methanol ( $-20^\circ\text{C}$ ) for 2 min and again left to dry. Then the samples were stained for 5 min with Congo Red (0.5% in PBS/0.01% NaOH), washed with PBS and left to dry. Then the coverslips were mounted in Vectashield before analysis on a Zeiss light-microscope equipped with a polarization filter to analyze the Congo Red birefringence.

### 2.5. Electron microscopy

$A\beta_{1-42}$  preparations were adsorbed onto formvar-coated 300-mesh copper grids for 5 min and excess fluid was filtered off. Subsequently, the samples were stained with 1% uranyl acetate for 5 min, excess fluid was filtered off and the grids were analyzed with a Philips EM-420 transmission electron microscope operated at 100 kV. The grids were thoroughly examined to get an overall evaluation of

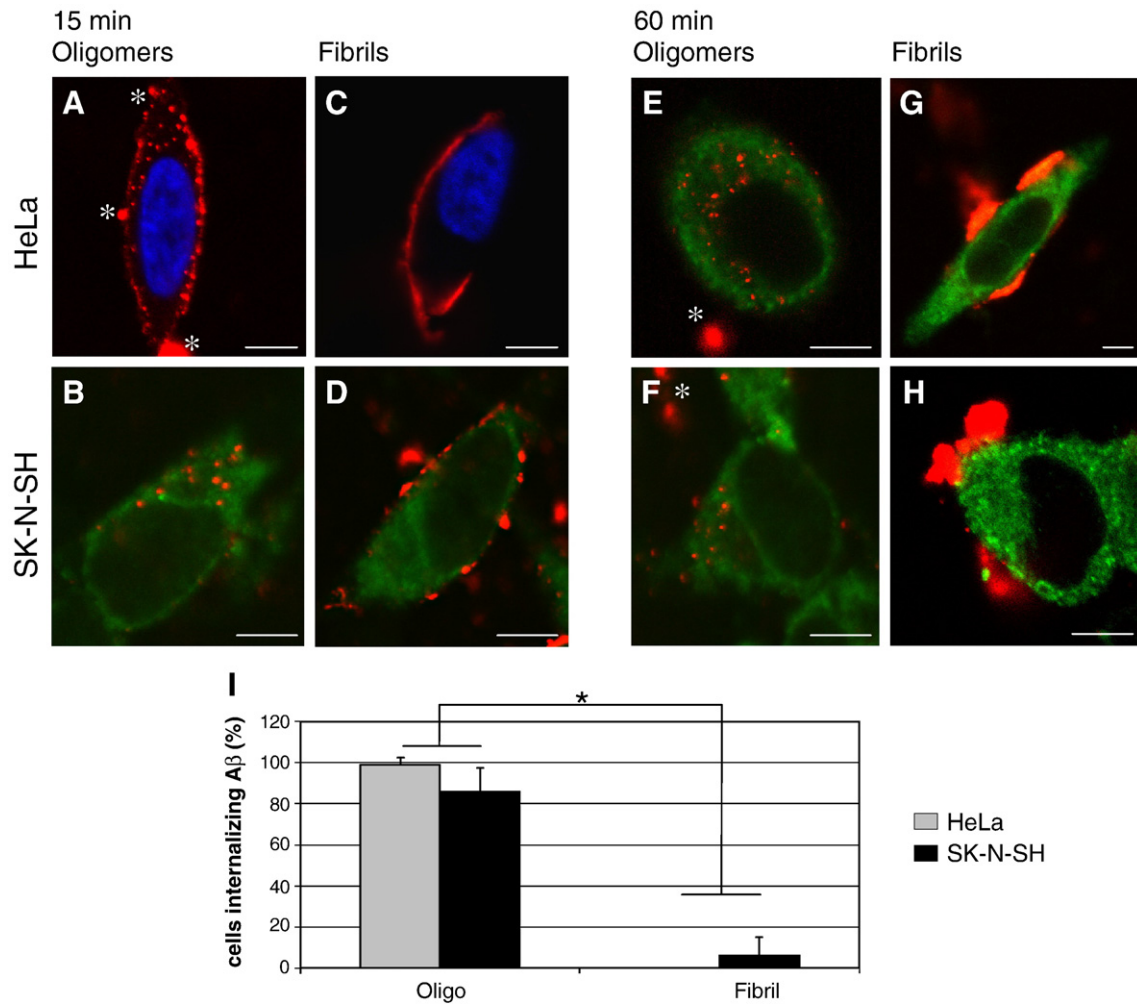


**Fig. 2.** Aggregation state dependent internalization of  $A\beta_{1-42}$ . Shown are confocal images from HeLa cells (A, C, E, G) and differentiated SK-N-SH cells (B, D, F, H) treated with either 10  $\mu$ M oligomeric preparations of TMR- $A\beta_{1-42}$  for 15 15 min (A, B) or 60 60 min (E, F) or 10  $\mu$ M fibrillar preparations for 15 15 min (C, D) or 60 60 min (G, H). After fixation, cells were counterstained with DAPI (blue in A, C) or a Calnexin antibody (green in B, D–H). Asterisks indicate TMR- $A\beta_{1-42}$  in the oligomeric preparation not internalized by the cells. Scale bar: 8  $\mu$ m. (I) HeLa cells and differentiated SK-N-SH cells were treated with 10  $\mu$ M TMR- $A\beta_{1-42}$  oligomers or fibrils for 15 15 min. For quantitative analysis of the HeLa cells 12 confocal images from 3–4 independent experiments (>100 cells in total) were counted. For quantitative analysis of the SK-N-SH cells 18–25 confocal images from 7–9 independent experiments (>200 cells in total) were counted. The graph represents the mean  $\pm$  S.D. from these experiments, the count for uptake of fibrillar  $A\beta_{1-42}$  in HeLa cells was 0; \* $p$ <0.001 (Student's *t*-test).

the structures present in the sample. Using the AnalySIS © software the diameters of the fibrils on the EM pictures were measured.

## 2.6. MTT assay

The cytotoxicity of the  $A\beta_{1-42}$  preparations was assessed by the 3-(4,5-dimethylthiazol-2-yl)-2,5-diphenyltetrazolium bromide (MTT) assay. Differentiated SK-N-SH or HeLa cells were incubated with 10  $\mu$ M oligomeric or fibrillar TMR- $A\beta_{1-42}$  or unlabelled  $A\beta_{1-42}$  preparations for the indicated times. Following the treatments, cells were incubated with MTT (0.25 25 mg/ml) for 2 h at 37 °C and the formazan salt generated by viable cells as a result of conversion of MTT was dissolved in DMSO and the absorbance was measured at 570 570 nm. In some experiments, HeLa cells and differentiated SK-N-SH cell were incubated for 30 30 min with 5 5 mM and 1 1 mM methyl- $\beta$ -cyclo-dextrin (M $\beta$ CD), respectively, prior to  $A\beta_{1-42}$  treatment. Experiments were performed at least twice, in triplicate.

## 2.7. Confocal and immunofluorescence microscopy

Uptake of  $A\beta$  and the subcellular localization of  $A\beta$  was assessed by confocal microscopy, using a Leica TCS-SP2 mounted on an

inverted microscope (Leica, Heidelberg, Germany) or by immunofluorescence microscopy (Olympus AH3 Vanox) both equipped with a digital CCD camera. Differentiated neuroblastoma SK-N-SH cells and HeLa cells were grown on non-coated sterile glass coverslips. Cells were treated with 10  $\mu$ M oligomeric or fibrillar TMR-labelled  $A\beta_{1-42}$  for 15 min. To study the involvement of endocytosis in  $A\beta$  uptake, cells were co incubated with TMR  $A\beta$  and Alexa488 labelled Tfn. Therefore cells were incubated for 30 min with serum-free medium to deplete the cells from Tfn normally present in serum-containing medium, prior to co-incubation with  $A\beta$  and the fluorescent Tfn-probe for 15 min. For endocytosis inhibitor experiments HeLa and differentiated SK-N-SH cells were pre treated with 5 mM and 1 mM M $\beta$ CD, respectively, for 30 min. Subsequently, the M $\beta$ CD was washed away and the cells were incubated in serum free medium for 30 min followed by 15 min incubation with Alexa488-labelled Tfn (40  $\mu$ g/ml in serum free medium). Then the cells were washed twice with cell culture medium, fixed with 4% paraformaldehyde for 20 min at room temperature and were incubated with DAPI and mounted in Vectashield, in case of counterstaining with calnexin, after permeabilization with 0.05% saponin in PBS, and primary and secondary antibody incubations in 0.05% saponin/1.0 % BSA in PBS.

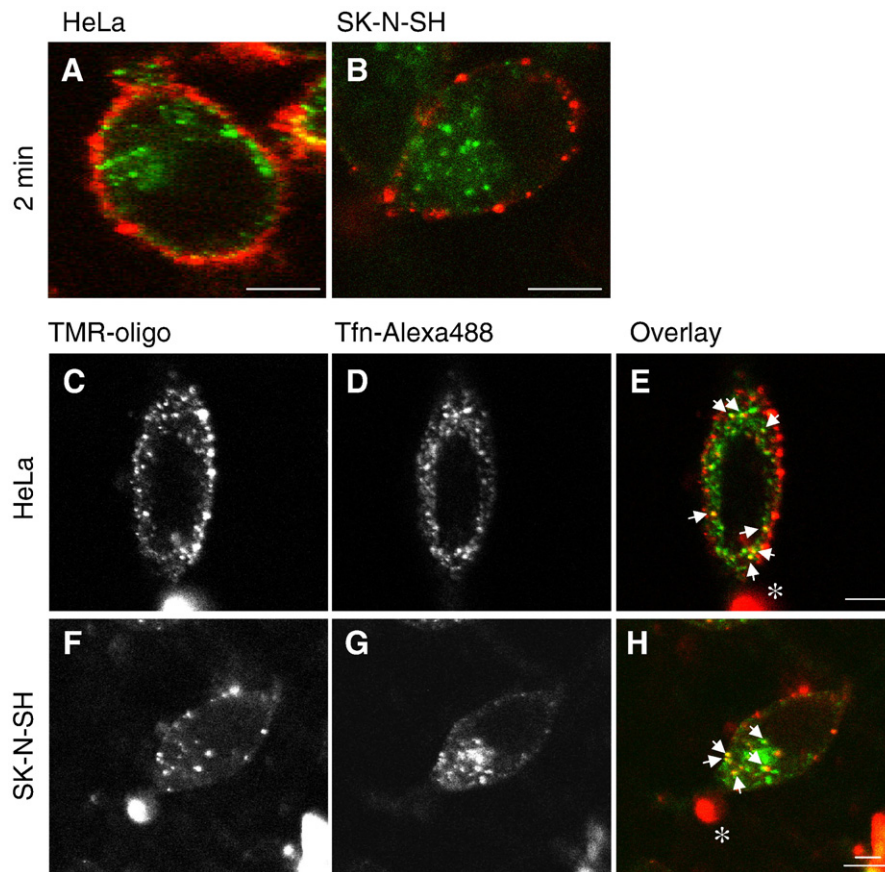


**Fig. 3.**  $A\beta_{1-42}$  oligomers are internalized via endocytosis. Differentiated SK-N-SH cells or HeLa cells were co incubated with 10  $\mu\text{M}$  oligomeric TMR- $A\beta_{1-42}$  and 40  $\mu\text{g}/\text{ml}$  Alexa488-Tfn for different times. (A, B) Confocal images from HeLa (A) and differentiated SK-N-SH (B) cells treated with oligomeric preparations of TMR- $A\beta_{1-42}$  for 2 min. TMR- $A\beta_{1-42}$  oligomers are not internalized after 2 min. (C–H) Confocal images from HeLa cells (C–E) and differentiated SK-N-SH (F–H) treated with TMR- $A\beta_{1-42}$  oligomers (C, F) in presence of Alexa-488-Tfn (D, G) for 15 min. Yellow signal (arrows) in the overlay pictures (E, H) shows partial co-localization of  $A\beta$  with endosomes. TMR- $A\beta_{1-42}$  oligomers are internalized after 15 min. Asterisks indicate larger aggregates in the oligomeric preparation not internalized by the cells. Scale bar: 5  $\mu\text{m}$ .

To study the possible involvement of lysosomes in  $A\beta$  trafficking, we used LysoTracker Green for fluorescent labelling of lysosomes in live cells. Cells were incubated with TMR-labelled  $A\beta$  oligomers for the indicated times. Subsequently the cells were treated with 50 nM LysoTracker Green for 5 min. Live cells were imaged on a confocal microscope using an objective heater (set at 37  $^{\circ}\text{C}$ ). All microscopy experiments have been conducted at least twice with different  $A\beta$  preparations.

All microscopy experiments have been conducted at least twice with different  $A\beta$  preparations.

### 3. Results

#### 3.1. Structural and biological properties of TMR- $A\beta_{1-42}$

Previously, it was shown that the N-terminus of  $A\beta$  is more accessible and less involved in fibrillogenesis than other regions of the sequence [23], thus a fluorescent group at the N-terminus is less likely to interfere with  $A\beta$  aggregation than a fluorescent group at the C-terminus. Therefore we used  $A\beta_{1-42}$  that was N-terminally labelled with the red fluorophore tetramethylrhodamine (TMR- $A\beta_{1-42}$ ) to make oligomer- and fibril-enriched preparations. TMR- $A\beta_{1-42}$  was mixed with 2 molar equivalents of unlabelled  $A\beta_{1-42}$  to minimize possible interference of the fluorophore with aggregation whilst retaining sufficient fluorescent signal. This mixture is used as TMR- $A\beta_{1-42}$  throughout the experiments.

To characterize the structural and biological features of TMR- $A\beta_{1-42}$ , the aggregation and toxic properties were compared to those of

unlabelled  $A\beta_{1-42}$ . Fibrillar and oligomeric preparations of both TMR- $A\beta_{1-42}$  as well as unlabelled  $A\beta_{1-42}$  were analyzed using negative stain on transmission electron microscopy (TEM, Fig. 1A–D). Both types of oligomers appeared as small globular structures (with an average diameter of approximately 5.5 nm) on electron micrographs, in good accordance with the size reported by others using a similar protocol for oligomer preparation [16,17,24,25]. In the fibrillar preparations, both TMR- $A\beta_{1-42}$  and unlabelled fibrils showed long threads measuring  $>1 \mu\text{m}$  in length, in line with reported lengths for  $A\beta$  fibrils [6,16,17,26]. In addition, the diameter of the labelled and unlabelled fibrils as measured on EM showed no significant difference ( $7.4 \pm 1.41$  and  $7.6 \pm 1.45$  nm, respectively, Fig. 1E) and are in line with the reported width of  $A\beta$  fibrils [6,16,17,26]. EM analysis thus indicates that the fluorescent group does not interfere with the ultrastructure of  $A\beta$  aggregates. To obtain information about the  $\beta$ -sheet content of the fibrils, Congo Red (CR) staining was performed. Both fibril types showed CR binding (Fig. 1F, G) as well as birefringence under polarized light (Fig. 1H, I), indicating that the TMR group does not interfere with stacking in the fibrils.

Next we compared the toxic properties of TMR- $A\beta_{1-42}$  and unlabelled  $A\beta_{1-42}$  in differentiated SK-N-SH cells. The decrease in viability of SK-N-SH cells caused by fibrillar TMR- $A\beta_{1-42}$  ( $82.3 \pm 9.2\%$ ) and unlabelled fibrils ( $85.4 \pm 5.2\%$ ) was not significantly different. Although the decrease in viability of SK-N-SH caused by 10  $\mu\text{M}$  oligomeric TMR- $A\beta_{1-42}$  ( $62.3 \pm 3.5\%$ ) is slightly lower compared to 10  $\mu\text{M}$  unlabelled oligomers ( $57.3 \pm 2.8\%$ ), the differential toxicity between oligomeric and fibrillar  $A\beta_{1-42}$  that was reported previously [16,21], is retained (Fig. 1J). Based on the combination of structural

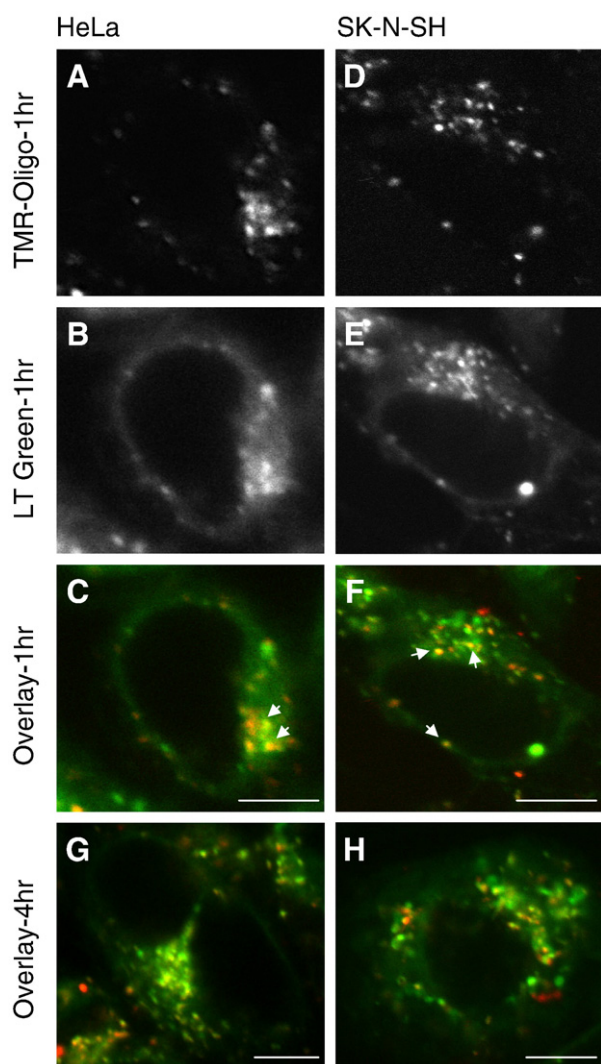


**Fig. 4.** Internalized  $A\beta_{1-42}$  oligomers is targeted to lysosomes. HeLa cells (A–C, G) and differentiated SK-N-SH cells (D–F, H) were treated with  $10 \mu\text{M}$  TMR- $A\beta_{1-42}$  oligomers for 1 h (A–F) or 4 h (G–H) and subsequently incubated with  $50 \text{ nM}$  LysoTracker (LT) Green. Merged confocal images (C, F, G, H) present TMR- $A\beta_{1-42}$  oligomers in red, LT in green and co-localization of  $A\beta$  oligomers with lysosomes in yellow (arrows). Scale bar:  $10 \mu\text{m}$ .

(EM/CR) and biological data, we conclude that oligomeric and fibrillar TMR-labelled  $A\beta_{1-42}$  have similar structural and toxic properties as unlabelled  $A\beta_{1-42}$ . Therefore TMR-labelled  $A\beta_{1-42}$  provides a valid model to study aggregation state specific effects on the subcellular localization of  $A\beta_{1-42}$ .

### 3.2. Aggregation state specific uptake of $A\beta_{1-42}$

To investigate whether oligomeric and fibrillar  $A\beta_{1-42}$  are differentially internalized, cells were treated for 15 min with either TMR-oligomers or TMR fibrils. After treatment the cells were fixed and counterstained with anti-Calnexin (to visualize the ER) or DAPI (to label the nucleus). We used HeLa cells and differentiated SK-N-SH cells, the latter to provide a more neuronal model of non dividing cells. In cells treated with oligomers, intracellular red spots are observed distributed throughout the cell body of both HeLa and SK-N-SH cells after 15 min, indicating that the oligomeric  $A\beta_{1-42}$  is internalized (Fig. 2A, B). In contrast, in cells treated with TMR-fibrils, all fluorescent signals are located at the cell surface (Fig. 2C, D). This indicates specific uptake of oligomeric  $A\beta$  in both cell types. Uptake of oligomeric  $A\beta$  is not a chance event, as it observed in essentially

every cell (Fig. 2I). In SK-N-SH cells treated with  $A\beta_{1-42}$  oligomers,  $86.0 \pm 11.3\%$  internalized  $A\beta$ , whereas only  $6.1 \pm 9.0\%$  of the cells treated with  $A\beta_{1-42}$  fibrils showed the presence of  $A\beta$  inside the cell. The difference in the internalization of fibrils and oligomers is even more pronounced in HeLa cells. Whereas not a single HeLa cell detectably internalizes fibrillar  $A\beta_{1-42}$ , virtually all cells ( $99.0 \pm 3.6\%$ ) internalize  $A\beta_{1-42}$  oligomers (Fig. 2I). Some of the oligomeric material appears to remain outside the cell (Fig. 2A, indicated by asterisks throughout the figures) and is also observed at later time points (e.g. Fig. 2E and F) This material is often localized at or close to the plasma membrane and is larger in size than the internalized  $A\beta$  and may represent a larger aggregated form. Our results show that both cell types internalize  $A\beta$  oligomers, whereas fibrillar  $A\beta$  is located only at the cell surface. After prolonging the incubation time of TMR-labelled fibrils up to an hour, still no intracellular fluorescent signal is observed, whereas the TMR oligomers are abundantly present intracellularly (Fig. 2E–H), indicating that the cells are not capable of internalizing fibrillar  $A\beta_{1-42}$  aggregates.

### 3.3. Uptake of $A\beta_{1-42}$ oligomers via endocytosis

To study if the uptake of  $A\beta$  oligomers occurs via endocytosis we used fluorescently labelled transferrin (Alexa-488 Tfn) as a marker for endocytosis. After depletion of Tfn in serum free cell culture medium, HeLa and differentiated SK-N-SH cells were co-incubated with TMR- $A\beta$  oligomers and Alexa488-Tfn in serum-free medium. Although Tfn has entered the cells after 2 min, TMR-labelled oligomers are localized at the cell surface and are not found in the intracellular space (Fig. 3A, B). This is still the case at 5 min (not shown), but after 15 min oligomeric  $A\beta$  was observed inside the cell as shown before (Fig. 2). This internalized  $A\beta$  partially co-localizes with Tfn in both cell types (Fig. 3C–H). This indicates that  $A\beta$  is at least partly internalized by endocytosis in both HeLa and SK-N-SH cells, however, uptake of  $A\beta$  oligomers takes longer than uptake of fluorescent Tfn.

### 3.4. $A\beta_{1-42}$ oligomers end up in lysosomes

To determine the subcellular destination of  $A\beta$  after uptake, we performed further co-localizations. We find no co-localization of  $A\beta$  with the ER or the Golgi, also not after prolonged incubation up to 4 and 24 h, respectively (not shown). This indicates that following endocytosis, oligomeric  $A\beta_{1-42}$  is not retrogradely transported to the compartments of the early secretory pathway. The most likely candidate for transport from the endosomes is the lysosomal compartment. Differentiated SK-N-SH and HeLa cells were treated for the indicated times with TMR- $A\beta_{1-42}$  oligomers, and subsequently LysoTracker Green was added to visualize lysosomes in living cells on a confocal microscope. After 1 h we observed partial co-localization of TMR-labelled oligomers and LysoTracker Green (Fig. 4A–F). After 4 h, the co-localization of the  $A\beta_{1-42}$  oligomers with LysoTracker is still observed in both cell types, indicating that  $A\beta_{1-42}$  is not rapidly degraded in the lysosomes, (Fig. 4G, H). This result suggests that after endocytosis,  $A\beta_{1-42}$  oligomers are subsequently transported to the lysosomal compartment.

### 3.5. Inhibition of $A\beta$ uptake inhibits oligomer specific toxicity

To test whether selective uptake of oligomers can explain the higher toxicity of oligomers compared to fibrils,  $A\beta$  treatment was performed in the presence of the general endocytosis inhibitor methyl- $\beta$ -cyclodextrin (M $\beta$ CD). Co-localization with Alexa488-Tfn-containing endosomes may indicate that  $A\beta$  oligomers are internalized by clathrin-mediated endocytosis (similar to Tfn). It has been shown previously, however, that molecules that are internalized via clathrin-independent mechanisms reach the same early and late endosome as encountered by molecules internalized via clathrin coated pits [27]. Therefore we used the drug M $\beta$ CD, which extracts

cholesterol from the membrane, thereby inhibiting both caveolae- and clathrin-dependent endocytosis [28–30]. HeLa cells were treated with 10  $\mu$ M oligomeric or fibrillar A $\beta_{1-42}$  for 4 h following a pre-treatment with 5 mM M $\beta$ CD or vehicle for 30 min. This strongly inhibits the

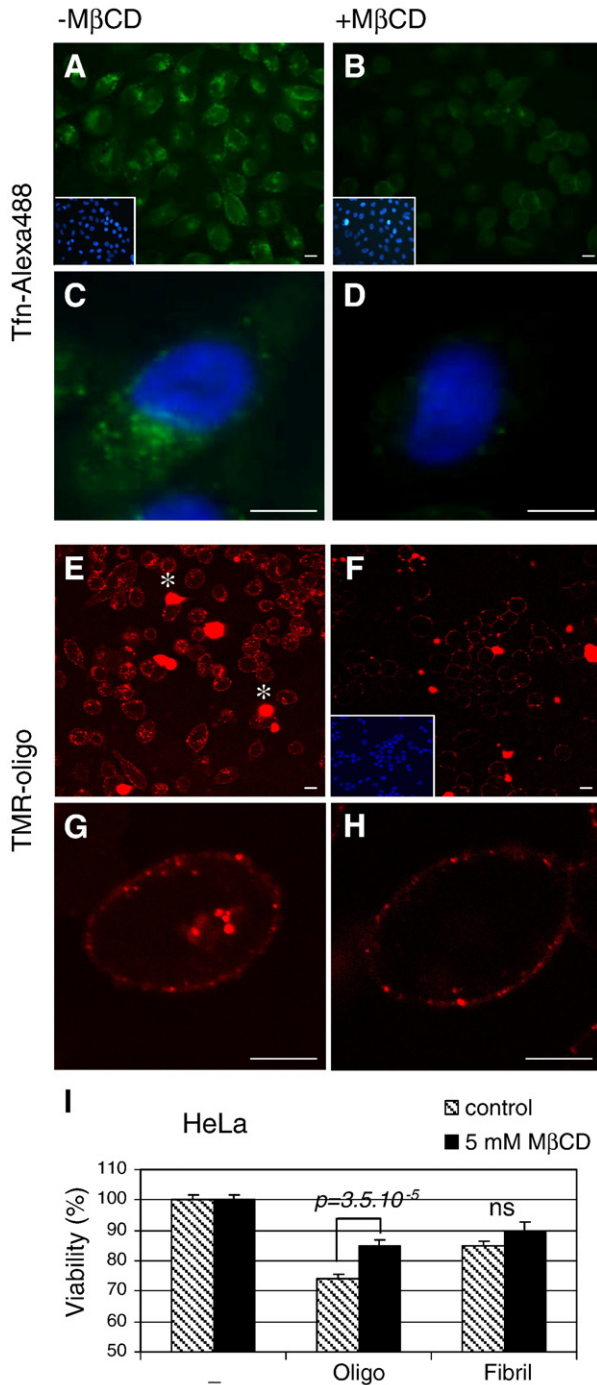


**Fig. 5.** Uptake of A $\beta_{1-42}$  oligomers contributes to A $\beta$  oligomer specific toxicity in HeLa cells. HeLa cells were treated with 40  $\mu$ g/ml Alexa488-Tfn or 10  $\mu$ M TMR-A $\beta_{1-42}$  oligomers for 15 min following a pretreatment in absence (A, C, E, G) or presence (B, D, F, H) of 5 mM M $\beta$ CD for 30 min. Immunofluorescence pictures (A–D) demonstrating inhibition of endocytosis of Alexa488-Tfn after M $\beta$ CD treatment and confocal pictures (E–H) showing inhibition of uptake of TMR-A $\beta_{1-42}$  oligomers (insets show nuclei of HeLa cells stained with DAPI) Asterisks indicate larger aggregates in the oligomeric preparation not internalized by the cells. Scale bars: 10  $\mu$ m. (I) HeLa cells were treated with 10  $\mu$ M A $\beta$  oligomers or fibrils for 4 h following a pre-treatment in presence or absence of 5 mM M $\beta$ CD for 30 min. Shown is a representative graph of an MTT assay. Viability (mean  $\pm$  S.D. from  $n=3$ ) is depicted as percentage of cells without A $\beta$ . Statistically significant differences (Student's  $t$ -test) are indicated.

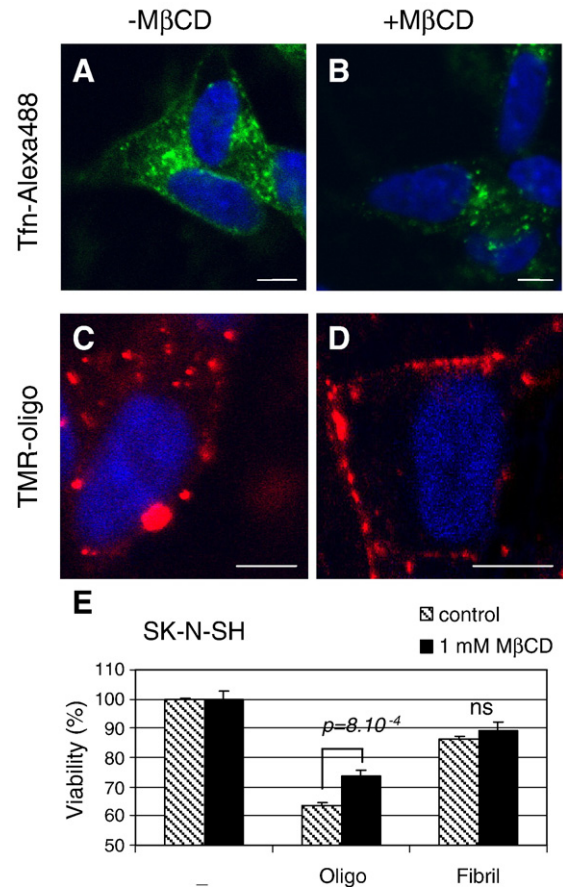


**Fig. 6.** Uptake of A $\beta_{1-42}$  oligomers contributes to A $\beta$  oligomer specific toxicity in SK-N-SH cells. Differentiated SK-N-SH cells were treated with 40  $\mu$ g/ml Alexa488-Tfn or 10  $\mu$ M TMR-A $\beta_{1-42}$  oligomers for 15 min following a pretreatment in absence (A, C) or presence (B, D) of 1 mM M $\beta$ CD for 30 min. Immunofluorescence pictures (A, B) and confocal pictures (C, D) demonstrate inhibition of endocytosis of Alexa488-Tfn and uptake of TMR-A $\beta_{1-42}$  oligomers by M $\beta$ CD treatment, respectively. Cells are counterstained with DAPI (blue). Scale bars: 10  $\mu$ m. (E) Differentiated SK-N-SH cells were treated with 10  $\mu$ M A $\beta$  oligomers or fibrils for 4 h following a pre treatment in presence or absence of 1 mM M $\beta$ CD for 30 min. Shown is a representative graph of an MTT assay. Viability (mean  $\pm$  S.D. from  $n=3$ ) is depicted as percentage of cells without A $\beta$ . Statistically significant differences (Student's  $t$ -test) are indicated.

uptake of fluorescent Tfn, indicating a near complete inhibition of endocytosis (Fig. 5A–D). In the same experimental set up, A $\beta$  uptake is nearly abolished and is found at the plasma membrane (Fig. 5E–H). Using the MTT viability assay, the effect of inhibition of uptake on A $\beta$  toxicity was analysed. In absence of M $\beta$ CD a significant difference in toxicity of oligomers compared to fibrils (Fig. 5I, viability 74% and 84%, respectively,  $p < 0.001$ ) is observed, although less pronounced than in the differentiated SK-N-SH cells (Fig. 1J). We find that M $\beta$ CD pretreatment increases the viability of cells treated with A $\beta$  oligomers to 85%, whereas the viability of fibril treated cells is unaffected (Fig. 5I), thereby losing the differential effect on cell viability of oligomers and fibrils. The SK-N-SH cells do not tolerate this concentration of M $\beta$ CD, therefore these cells were treated with a lower concentration (1 mM). Under these conditions, Tfn uptake is not completely inhibited (Fig. 6A, B), but the uptake of A $\beta$  oligomers is strongly inhibited (Fig. 6C, D), albeit to a lesser extent than in the HeLa cells with the higher concentration of M $\beta$ CD that shows stronger inhibition of endocytosis altogether. In the differentiated SK-N-SH as well, M $\beta$ CD significantly reduces the toxicity of oligomeric A $\beta$  (viability from 63% to 74%  $p < 0.001$ ), but does not affect the viability of cells treated with fibrillar A $\beta$  (Fig. 6E).

#### 4. Discussion

In the present study we investigated whether different accessibility to the intracellular space can underlie the differential effects of oligomeric and fibrillar  $A\beta_{1-42}$  on cellular toxicity. To study interactions of  $A\beta$  oligomers and fibrils with cells, we used N-terminally TMR-labelled  $A\beta$  to generate preparations enriched in oligomeric or fibrillar  $A\beta$  using an established protocol [16,18,21]. Our data corroborate other studies where different fluorophores at the N-terminus of  $A\beta$  also showed little effect on the amyloidogenic properties of  $A\beta$  [31–33]. We show no effect of the fluorophore on oligomer or fibril morphology nor on the ability to form  $\beta$ -sheets. In addition our data show that the fluorophore does not affect the difference in toxicity between oligomeric and fibrillar preparations. Therefore we consider the TMR- $A\beta_{1-42}$  a valid model to study aggregation-state specific effects of  $A\beta_{1-42}$ .

Both in HeLa and differentiated SK-N-SH cells, we found that oligomeric TMR- $A\beta_{1-42}$  is internalized whereas fibrillar TMR- $A\beta_{1-42}$  remains outside, even after prolonged incubation. We find similar results in HEK293 cells and MeJuSo cells (data not shown). This indicates that the aggregation state dependent uptake is not cell-type specific, although phagocytic cells like microglia and macrophages, have been shown to be able to phagocytose fibrillar  $A\beta$  [34,35]. It is possible that the presence of  $A\beta$  in the relatively compact fibrillar structure precludes exposure of amino acids required for interaction with a specific receptor. Another likely explanation for the aggregation state dependent uptake of  $A\beta$  may be the 3-dimensional characteristics of the aggregate. Uptake of particles into mammalian cells is size and shape dependent as was determined using gold nanoparticles. Most efficient uptake was found with small (50 nm), spherical gold nanoparticles. Increasing particle size greatly reduces its uptake. Uptake of rod-shaped particles also occurs at a much lower rate [36,37]. Oligomers are spherical  $A\beta$  structures with an average z height and diameter of 5 nm [4] and thus have structural features that facilitate uptake in the cell. In contrast, fibrils are rod-shaped structures over 1  $\mu$ m in length with a diameter of 7 nm, structural properties not compatible with easy internalization. Not all  $A\beta$  in the oligomer preparation is internalized. In oligomer-treated samples, particles are observed on the outside of the cell membrane that are typically much larger than the internalized material. Since  $A\beta$  aggregation has been shown to occur very rapidly in the presence of lipid bilayers, such as lipid rafts [38–42], this material may represent larger aggregates formed during the incubation with the cells, that can no longer be internalized. These larger aggregates are most likely not fibrils, since it was shown previously that oligomeric preparations similar to ours do not form fibrils for several days even not during incubation at 37 °C [4].

To study if oligomers are specifically internalized by the cell via endocytosis, cells were co-incubated with TMR-oligomers in presence of Alexa488-Tfn. Transferrin binds to the transferrin receptor and this complex is internalized via receptor mediated endocytosis. Both in HeLa cells and differentiated SK-N-SH cells  $A\beta$  oligomers were internalized at least in part via endocytosis, as shown by the co-localization of TMR- $A\beta$  oligomers and Alexa488-Tfn. The Tfn-probe only labels early and recycling endosomes, since the Tfn receptor/Tfn complex is recycled back to the plasma membrane [43]. Therefore the  $A\beta$  not co-localizing with Tfn is most likely present in late endosomes or other compartments beyond early endosomes. Alternatively,  $A\beta$  oligomers are in an endosome that does not contain Alexa488-Tfn. Partial co-localization may be caused by differential endocytic sorting of Tfn, that is recycled via recycling endosomes and  $A\beta$ , that is transported to the lysosomal compartment. Internalized LDL (low-density lipoprotein), that is (like TMR- $A\beta$  oligomers) transported to the lysosomes also shows only partial co-localization with Tfn [44]. Pre-treatment with an endocytosis inhibitor, M $\beta$ CD, strongly inhibits both Tfn and  $A\beta$  uptake, confirming endocytosis as mechanism of  $A\beta$  uptake. Endocytosis of  $A\beta$  oligomers occurs at a slower rate (15 min)

than endocytosis of Tfn (<2 min). This is most likely due to the fact that Tfn, has a highly specific receptor (Tfn-receptor) to which it binds very efficiently, leading to fast uptake by the cell. The binding of  $A\beta$  to the plasma membrane has been studied previously, and a number of candidate  $A\beta$ -binding receptors have been identified (such as FPRL1-, RAGE-, NMDA- and LRP-receptors [8]). However, none of these receptors is designed for the uptake of  $A\beta$  oligomers and their affinity for  $A\beta$  may be lower than for their natural ligands. For example, binding of  $A\beta$  to the  $\alpha$ 7 nicotinic acetylcholine receptor results in internalization and accumulation of  $A\beta$  intracellularly [45,46].  $A\beta$  internalization via the  $\alpha$ 7 nicotinic receptor occurs after 30 min [45], whereas its natural ligand nicotine is endocytosed within 5 min [47].

Not surprisingly we found  $A\beta_{1-42}$  oligomers clearly present in lysosomes. Increased accumulation of  $A\beta_{1-42}$  oligomers in the lysosomal compartment after longer incubation, suggests that its presence in the lysosome is involved in toxicity. This is in accordance with other studies showing presence of  $A\beta_{1-42}$  in the endosomal/lysosomal system [48–50].  $A\beta_{1-42}$  is poorly degraded by lysosomes [51] and its accumulation in lysosomes of cultured neurons causes leakage of lysosomal enzymes [52] and can ultimately lead to programmed cell death [53]. This may explain the toxicity that we observe after endocytosis and subsequent accumulation in the lysosomes and may be one of the pathways leading to neurodegeneration in AD. This is supported by data from post mortem brain material: neurons in vulnerable brain regions in AD patients show an increased number of structurally abnormal endosomes and lysosomes, endosome enlargement, and an increase in expression of lysosomal hydrolases [51,54,55]. In addition to these direct toxic effects, the endosomal-lysosomal pathway has been identified as particularly important to processing of the amyloid precursor protein (APP) [56–60]. In case the endosomal-lysosomal compartment is compromised by  $A\beta$  this can lead to redistribution of APP and its processing activities and thus increase  $A\beta$  production. Endosomal/lysosomal abnormalities are therefore believed to contribute significantly to  $A\beta$  overproduction [57,61,62] and neuronal dysfunction [9]. The presence of  $A\beta_{1-42}$  in the endosomal-lysosomal system can thus lead to an autocatalytic cycle that results in an increase in the levels of  $A\beta$ , that in turn can aggregate and is poorly degraded [63].

To determine if there is a connection between subcellular localization and  $A\beta$  toxicity, toxicity of oligomers in absence or presence of M $\beta$ CD was compared. Inhibition of uptake reduces the toxicity of oligomers in both HeLa as well as differentiated SK-N-SH cells. The toxicity of fibrillar  $A\beta_{1-42}$  is not affected, which is in good accordance with the lack of internalization of fibrils. In the differentiated SK-N-SH cells a total block of uptake was not tolerated, but even incomplete inhibition relieved oligomer-specific toxicity. Interestingly, in HeLa cells, the M $\beta$ CD treatment reduced the oligomer toxicity to a level similar to that of fibrils. This indicates that  $A\beta_{1-42}$  can exert toxicity from the outside of the cell (i.e. the toxicity of fibrils and the residual toxicity of oligomers present at or close to the plasma membrane, after inhibition of uptake), but that for the specific toxicity of oligomeric  $A\beta_{1-42}$  uptake is required. A recent study by Bateman et al. shows that a cell line that is resistant to  $A\beta$  cytotoxicity, the non neuronal human lymphoma cell line U937 [64], does not bind  $A\beta_{1-42}$  [33]. This suggests that at least an interaction of  $A\beta$  with the cell membrane is required to confer toxicity on mammalian cells. An alternative explanation for the protective effect of M $\beta$ CD could be that once depleted of cholesterol, membranes are less susceptible to oligomers. Conflicting results have been reported so far on the effects of cholesterol enrichment and depletion from the plasma membrane on  $A\beta$  toxicity and membrane binding [38,65–69]. The experimental design in these studies was not optimal to fully explore  $A\beta$  toxicity following M $\beta$ CD treatment, because cell viability was determined after 24 h or longer, giving the cell time to replenish the cholesterol levels of the membrane. This makes it difficult to interpret these results on the role of cholesterol on  $A\beta$  toxicity. Regardless, decreased

membrane binding does not provide a likely explanation for the protective effect we observe of M $\beta$ CD treatment, since we find that the majority of A $\beta$  oligomers is membrane associated after pre-treatment with M $\beta$ CD.

There is a large body of evidence demonstrating that A $\beta$  accumulates intracellularly and that A $\beta$  accumulation inside neurons is detrimental to a range of cellular processes [8]. It is unclear whether the intracellular A $\beta$  accumulates because part of the intracellularly generated A $\beta$  is not secreted, or whether it derives from re-uptake of secreted A $\beta$ . Several studies indicate that intra- and extracellular pools are in equilibrium, as clearance of extracellular A $\beta$  depletes the intracellular pool as well [70]. Therefore, targeting of the more easily accessible extracellular A $\beta$  is still a promising option for therapeutic intervention. We report here that selective uptake of oligomeric A $\beta$  contributes to toxicity. Our study indicates that prevention of the internalization of oligomeric A $\beta$  may be an attractive additional aim in therapeutic strategies targeting extracellular A $\beta$ .

### Acknowledgements

We would like to thank Dr. Jeroen Hoozemans and Prof. Piet Eikelenboom for the stimulating discussions. This work is supported by: the Internationale Stichting Alzheimer Onderzoek (ISAO grant 05508 and 07506), the European Commission as part of the 6th framework programme (EDAR), the Netherlands organization for Scientific Research (NWO Meervoud Grant 836.05.060).

### References

- [1] W. Annaert, B. De Strooper, A cell biological perspective on Alzheimer's disease, *Annu. Rev. Cell Dev. Biol.* 18 (2002) 25–51.
- [2] M. Hutton, J. Perez-Tur, J. Hardy, Genetics of Alzheimer's disease, *Essays Biochem.* 33 (1998) 117–131.
- [3] J.P. Taylor, J. Hardy, K.H. Fischbeck, Toxic proteins in neurodegenerative disease, *Science* 296 (2002) 1991–1995.
- [4] B.A. Chromy, R.J. Nowak, M.P. Lambert, K.L. Viola, L. Chang, P.T. Velasco, B.W. Jones, S.J. Fernandez, P.N. Lacor, P. Horowitz, C.E. Finch, G.A. Krafft, W.L. Klein, Self-assembly of Abeta(1–42) into globular neurotoxins, *Biochemistry* 42 (2003) 12749–12760.
- [5] C.J. Pike, D. Burdick, A.J. Walencewicz, C.G. Glabe, C.W. Cotman, Neurodegeneration induced by beta-amyloid peptides in vitro: the role of peptide assembly state, *J. Neurosci.* 13 (1993) 1676–1687.
- [6] B. Seilheimer, B. Bohrmann, L. Bondolfi, F. Muller, D. Stuber, H. Dobeli, The toxicity of the Alzheimer's beta-amyloid peptide correlates with a distinct fiber morphology, *J. Struct. Biol.* 119 (1997) 59–71.
- [7] W. Scheper, E.M. Hol, Protein quality control in Alzheimer's disease: a fatal saviour, *Curr. Drug Targets CNS Neurol. Disord.* 4 (2005) 283–292.
- [8] F.M. LaFerla, K.N. Green, S. Oddo, Intracellular amyloid-beta in Alzheimer's disease, *Nat. Rev. Neurosci.* 8 (2007) 499–509.
- [9] A.M. Cataldo, S. Petanceska, N.B. Terio, C.M. Peterhoff, R. Durham, M. Mercken, P.D. Mehta, J. Buxbaum, V. Haroutunian, R.A. Nixon, Abeta localization in abnormal endosomes: association with earliest Abeta elevations in AD and Down syndrome, *Neurobiol. Aging* 25 (2004) 1263–1272.
- [10] M.R. D'Andrea, R.G. Nagele, H.Y. Wang, P.A. Peterson, D.H. Lee, Evidence that neurones accumulating amyloid can undergo lysis to form amyloid plaques in Alzheimer's disease, *Histopathology* 38 (2001) 120–134.
- [11] C. Mori, E.T. Spooner, K.E. Wisniewski, T.M. Wisniewski, H. Yamaguchi, T.C. Saido, D.R. Tolan, D.J. Selkoe, C.A. Lemere, Intraneuronal Abeta42 accumulation in Down syndrome brain, *Amyloid* 9 (2002) 88–102.
- [12] J. Rodrigo, P. Fernandez-Vizarra, S. Castro-Blanco, M.L. Bentura, M. Nieto, T. Gomez-Isla, R. Martinez-Murillo, A. Martinez, J. Serrano, A.P. Fernandez, Nitric oxide in the cerebral cortex of amyloid-precursor protein (SW) Tg2576 transgenic mice, *Neuroscience* 128 (2004) 73–89.
- [13] L.M. Billings, S. Oddo, K.N. Green, J.L. McLaugh, F.M. LaFerla, Intraneuronal Abeta causes the onset of early Alzheimer's disease-related cognitive deficits in transgenic mice, *Neuron* 45 (2005) 675–688.
- [14] S. Oddo, L. Billings, J.P. Kesslak, D.H. Cribbs, F.M. LaFerla, Abeta immunotherapy leads to clearance of early, but not late, hyperphosphorylated tau aggregates via the proteasome, *Neuron* 43 (2004) 321–332.
- [15] P.T. Lansbury, H.A. Lashuel, A century-old debate on protein aggregation and neurodegeneration enters the clinic, *Nature* 443 (2006) 774–779.
- [16] K.N. Dahlgren, A.M. Manelli, W.B. Stine Jr., L.K. Baker, G.A. Krafft, M.J. LaDu, Oligomeric and fibrillar species of amyloid-beta peptides differentially affect neuronal viability, *J. Biol. Chem.* 277 (2002) 32046–32053.
- [17] M.P. Lambert, A.K. Barlow, B.A. Chromy, C. Edwards, R. Freed, M. Liosatos, T.E. Morgan, I. Rozovsky, B. Trommer, K.L. Viola, P. Wals, C. Zhang, C.E. Finch, G.A. Krafft, W.L. Klein, Diffusible, nonfibrillar ligands derived from Abeta1–42 are potent central nervous system neurotoxins, *Proc. Natl. Acad. Sci. U. S. A.* 95 (1998) 6448–6453.
- [18] R. Kaye, E. Head, J.L. Thompson, T.M. McIntire, S.C. Milton, C.W. Cotman, C.G. Glabe, Common structure of soluble amyloid oligomers implies common mechanism of pathogenesis, *Science* 300 (2003) 486–489.
- [19] D.M. Walsh, I. Klyubin, J.V. Fadeeva, W.K. Cullen, R. Anwyl, M.S. Wolfe, M.J. Rowan, D.J. Selkoe, Naturally secreted oligomers of amyloid beta protein potently inhibit hippocampal long-term potentiation in vivo, *Nature* 416 (2002) 535–539.
- [20] I. Klyubin, D.M. Walsh, C.A. Lemere, W.K. Cullen, G.M. Shankar, V. Betts, E.T. Spooner, L. Jiang, R. Anwyl, D.J. Selkoe, M.J. Rowan, Amyloid beta protein immunotherapy neutralizes Abeta oligomers that disrupt synaptic plasticity in vivo, *Nat. Med.* 11 (2005) 556–561.
- [21] S.M. Chafekar, J.J. Hoozemans, R. Zwart, F. Baas, W. Scheper, Abeta 1–42 induces mild endoplasmic reticulum stress in an aggregation state-dependent manner, *Antioxid. Redox. Signal* 9 (2007) 2245–2254.
- [22] P. Eikelenboom, C. Bate, W.A. Van Gool, J.J. Hoozemans, J.M. Rozemuller, R. Veerhuis, A. Williams, Neuroinflammation in Alzheimer's disease and prion disease, *Glia* 40 (2002) 232–239.
- [23] I. Kheterpal, A. Williams, C. Murphy, B. Bledsoe, R. Wetzel, Structural features of the Abeta amyloid fibril elucidated by limited proteolysis, *Biochemistry* 40 (2001) 11757–11767.
- [24] R.W. Hepler, K.M. Grimm, D.D. Nahas, R. Breese, E.C. Dodson, P. Acton, P.M. Keller, M. Yeager, H. Wang, P. Shughrue, G. Kinney, J.G. Joyce, Solution state characterization of amyloid beta-derived diffusible ligands, *Biochemistry* 45 (2006) 15157–15167.
- [25] R. Kaye, Y. Sokolov, B. Edmonds, T.M. McIntire, S.C. Milton, J.E. Hall, C.G. Glabe, Permeabilization of lipid bilayers is a common conformation-dependent activity of soluble amyloid oligomers in protein misfolding diseases, *J. Biol. Chem.* 279 (2004) 46363–46366.
- [26] R.V. Ward, K.H. Jennings, R. Jepras, W. Neville, D.E. Owen, J. Hawkins, G. Christie, J. B. Davis, A. George, E.H. Karran, D.R. Howlett, Fractionation and characterization of oligomeric, protofibrillar and fibrillar forms of beta-amyloid peptide, *Biochem. J.* 348 Pt 1 (2000) 137–144.
- [27] S.H. Hansen, K. Sandvig, B. van Deurs, Molecules internalized by clathrin-independent endocytosis are delivered to endosomes containing transferrin receptors, *J. Cell Biol.* 123 (1993) 89–97.
- [28] B. van Deurs, K. Roepstorff, A.M. Hommelgaard, K. Sandvig, Caveolae: anchored, multifunctional platforms in the lipid ocean, *Trends Cell Biol.* 13 (2003) 92–100.
- [29] S.K. Rodal, G. Skretting, O. Garred, F. Vilhardt, B. van Deurs, K. Sandvig, Extraction of cholesterol with methyl-beta-cyclodextrin perturbs formation of clathrin-coated endocytic vesicles, *Mol. Biol. Cell.* 10 (1999) 961–974.
- [30] A. Subtil, I. Gaidarov, K. Kobylarz, M.A. Lampson, J.H. Keen, T.E. McGraw, Acute cholesterol depletion inhibits clathrin-coated pit budding, *Proc. Natl. Acad. Sci. U. S. A.* 96 (1999) 6775–6780.
- [31] P. Sengupta, K. Garai, B. Sahoo, Y. Shi, D.J. Callaway, S. Maiti, The amyloid beta peptide (Abeta(1–40)) is thermodynamically soluble at physiological concentrations, *Biochemistry* 42 (2003) 10506–10513.
- [32] T.H. Huang, D.S. Yang, N.P. Plaskos, S. Go, C.M. Yip, P.E. Fraser, A. Chakrabarty, Structural studies of soluble oligomers of the Alzheimer beta-amyloid peptide, *J. Mol. Biol.* 297 (2000) 73–87.
- [33] D.A. Bateman, J. McLaurin, A. Chakrabarty, Requirement of aggregation propensity of Alzheimer amyloid peptides for neuronal cell surface binding, *BMC Neurosci.* 8 (2007) 29.
- [34] M. Fiala, J. Lin, J. Ringman, V. Kermani-Arab, G. Tsao, A. Patel, A.S. Lossinsky, M.C. Graves, A. Gustavson, J. Sayre, E. Sofroni, T. Suarez, F. Chiappelli, G. Bernard, Ineffective phagocytosis of amyloid-beta by macrophages of Alzheimer's disease patients, *J. Alzheimers Dis.* 7 (2005) 221–232 (discussion 255–62).
- [35] J. Koenigsnecht, G. Landreth, Microglial phagocytosis of fibrillar beta-amyloid through a beta1 integrin-dependent mechanism, *J. Neurosci.* 24 (2004) 9838–9846.
- [36] B.D. Chithrani, A.A. Ghazani, W.C. Chan, Determining the size and shape dependence of gold nanoparticle uptake into mammalian cells, *Nano Lett.* 6 (2006) 662–668.
- [37] B.D. Chithrani, W.C. Chan, Elucidating the mechanism of cellular uptake and removal of protein-coated gold nanoparticles of different sizes and shapes, *Nano Lett.* 7 (2007) 1542–1550.
- [38] M. Wakabayashi, T. Okada, Y. Kozutsumi, K. Matsuzaki, GM1 ganglioside-mediated accumulation of amyloid beta-protein on cell membranes, *Biochem. Biophys. Res. Commun.* 328 (2005) 1019–1023.
- [39] K. Matsuzaki, T. Noguchi, M. Wakabayashi, K. Ikeda, T. Okada, Y. Ohashi, M. Hoshino, H. Naiki, Inhibitors of amyloid beta-protein aggregation mediated by GM1-containing raft-like membranes, *Biochim. Biophys. Acta* 1768 (2007) 122–130.
- [40] T. Kawarabayashi, M. Shoji, L.H. Younkin, L. Wen-Lang, D.W. Dickson, T. Murakami, E. Matsubara, K. Abe, K.H. Ashe, S.G. Younkin, Dimeric amyloid beta protein rapidly accumulates in lipid rafts followed by apolipoprotein E and phosphorylated tau accumulation in the Tg2576 mouse model of Alzheimer's disease, *J. Neurosci.* 24 (2004) 3801–3809.
- [41] N. Yamamoto, Y. Fukata, M. Fukata, K. Yanagisawa, GM1-ganglioside-induced Abeta assembly on synaptic membranes of cultured neurons, *Biochim. Biophys. Acta* 1768 (2007) 1128–1137.
- [42] S.I. Kim, J.S. Yi, Y.G. Ko, Amyloid beta oligomerization is induced by brain lipid rafts, *J. Cell Biochem.* 99 (2006) 878–889.
- [43] F.R. Maxfield, T.E. McGraw, Endocytic recycling, *Nat. Rev. Mol. Cell Biol.* 5 (2004) 121–132.

- [44] R.N. Ghosh, D.L. Gelman, F.R. Maxfield, Quantification of low density lipoprotein and transferrin endocytic sorting HEP2 cells using confocal microscopy, *J. Cell Sci.* 107 (Pt 8) (1994) 2177–2189.
- [45] R.G. Nagele, M.R. D'Andrea, W.J. Anderson, H.Y. Wang, Intracellular accumulation of beta-amyloid(1–42) in neurons is facilitated by the alpha 7 nicotinic acetylcholine receptor in Alzheimer's disease, *Neuroscience* 110 (2002) 199–211.
- [46] H.Y. Wang, D.H. Lee, M.R. D'Andrea, P.A. Peterson, R.P. Shank, A.B. Reitz, beta-Amyloid(1–42) binds to alpha7 nicotinic acetylcholine receptor with high affinity. Implications for Alzheimer's disease pathology, *J. Biol. Chem.* 275 (2000) 5626–5632.
- [47] Z. Liu, A.W. Tearle, Q. Nai, D.K. Berg, Rapid activity-driven SNARE-dependent trafficking of nicotinic receptors on somatic spines, *J. Neurosci.* 25 (2005) 1159–1168.
- [48] D. Langui, N. Girardot, K.H. El Hachimi, B. Allinquant, V. Blanchard, L. Pradier, C. Duyckaerts, Subcellular topography of neuronal Abeta peptide in APPxPS1 transgenic mice, *Am. J. Pathol.* 165 (2004) 1465–1477.
- [49] N. Sasaki, S. Toki, H. Chowei, T. Saito, N. Nakano, Y. Hayashi, M. Takeuchi, Z. Makita, Immunohistochemical distribution of the receptor for advanced glycation end products in neurons and astrocytes in Alzheimer's disease, *Brain Res.* 888 (2001) 256–262.
- [50] A.J. Yang, D. Chandswangbhuvana, L. Margol, C.G. Glabe, Loss of endosomal/lysosomal membrane impermeability is an early event in amyloid Abeta1–42 pathogenesis, *J. Neurosci. Res.* 52 (1998) 691–698.
- [51] M.F. Knauer, B. Soreghan, D. Burdick, J. Kosmoski, C.G. Glabe, Intracellular accumulation and resistance to degradation of the Alzheimer amyloid A4/beta protein, *Proc. Natl. Acad. Sci. U. S. A.* 89 (1992) 7437–7441.
- [52] K. Ditaranto, T.L. Tekirian, A.J. Yang, Lysosomal membrane damage in soluble Abeta mediated cell death in Alzheimer's disease, *Neurobiol. Dis.* 8 (2001) 19–31.
- [53] G. Kroemer, M. Jaattela, Lysosomes and autophagy in cell death control, *Nat. Rev. Cancer* 5 (2005) 886–897.
- [54] A.M. Cataldo, C.M. Peterhoff, J.C. Troncoso, T. Gomez-Isla, B.T. Hyman, R.A. Nixon, Endocytic pathway abnormalities precede amyloid beta deposition in sporadic Alzheimer's disease and Down syndrome: differential effects of APOE genotype and presenilin mutations, *Am. J. Pathol.* 157 (2000) 277–286.
- [55] G.K. Gouras, J. Tsai, J. Naslund, B. Vincent, M. Edgar, F. Checler, J.P. Greenfield, V. Haroutunian, J.D. Buxbaum, H. Xu, P. Greengard, N.R. Relkin, Intraneuronal Abeta42 accumulation in human brain, *Am. J. Pathol.* 156 (2000) 15–20.
- [56] S.H. Pasternak, R.D. Bagshaw, M. Guiral, S. Zhang, C.A. Ackerley, B.J. Pak, J.W. Callahan, D.J. Mahuran, Presenilin-1, nicastrin, amyloid precursor protein, and gamma-secretase activity are co-localized in the lysosomal membrane, *J. Biol. Chem.* 278 (2003) 26687–26694.
- [57] P.M. Mathews, C.B. Guerra, Y. Jiang, O.M. Grbovic, B.H. Kao, S.D. Schmidt, R. Dinakar, M. Mercken, A. Hille-Rehfeld, J. Rohrer, P. Mehta, A.M. Cataldo, R.A. Nixon, Alzheimer's disease related overexpression of the cation-dependent mannose 6-phosphate receptor increases Abeta secretion: role for altered lysosomal hydrolase distribution in beta-amyloidogenesis, *J. Biol. Chem.* 277 (2002) 5299–5307.
- [58] O.M. Grbovic, P.M. Mathews, Y. Jiang, S.D. Schmidt, R. Dinakar, N.B. Summers-Terio, B.P. Ceresa, R.A. Nixon, A.M. Cataldo, Rab5-stimulated up-regulation of the endocytic pathway increases intracellular beta-cleaved amyloid precursor protein carboxyl-terminal fragment levels and Abeta production, *J. Biol. Chem.* 278 (2003) 31261–31268.
- [59] E.H. Koo, S.L. Squazzo, Evidence that production and release of amyloid beta-protein involves the endocytic pathway, *J. Biol. Chem.* 269 (1994) 17386–17389.
- [60] J.R. Cirrito, J.E. Kang, J. Lee, F.R. Stewart, D.K. Verges, L.M. Silverio, G. Bu, S. Mennerick, D.M. Holtzman, Endocytosis is required for synaptic activity-dependent release of amyloid-beta in vivo, *Neuron* 58 (2008) 42–51.
- [61] A.M. Cataldo, D.J. Hamilton, J.L. Barnett, P.A. Paskevich, R.A. Nixon, Abnormalities of the endosomal-lysosomal system in Alzheimer's disease: relationship to disease pathogenesis, *Adv. Exp. Med. Biol.* 389 (1996) 271–280.
- [62] R.A. Nixon, A.M. Cataldo, P.M. Mathews, The endosomal-lysosomal system of neurons in Alzheimer's disease pathogenesis: a review, *Neurochem. Res.* 25 (2000) 1161–1172.
- [63] A.J. Yang, M. Knauer, D.A. Burdick, C. Glabe, Intracellular A beta 1–42 aggregates stimulate the accumulation of stable, insoluble amyloidogenic fragments of the amyloid precursor protein in transfected cells, *J. Biol. Chem.* 270 (1995) 14786–14792.
- [64] M. Mazziotti, D.H. Perlmuter, Resistance to the apoptotic effect of aggregated amyloid-beta peptide in several different cell types including neuronal- and hepatoma-derived cell lines, *Biochem. J.* 332 (Pt 2) (1998) 517–524.
- [65] C. Cecchi, F. Rosati, A. Pensalfini, L. Formigli, D. Nosi, G. Liguri, F. Dichiaro, M. Morello, G. Danza, G. Pieraccini, A. Peri, M. Serio, M. Stefani, Seladin-1/DHCR24 protects neuroblastoma cells against Abeta toxicity by increasing membrane cholesterol content, *J. Cell Mol. Med.* (2008).
- [66] P. Ferrera, O. Mercado-Gomez, M. Silva-Aguilar, M. Valverde, C. Arias, Cholesterol potentiates beta-amyloid-induced toxicity in human neuroblastoma cells: involvement of oxidative stress, *Neurochem. Res.* (2008).
- [67] I. Sponne, A. Ffire, V. Koziel, T. Oster, J.L. Olivier, T. Pillot, Membrane cholesterol interferes with neuronal apoptosis induced by soluble oligomers but not fibrils of amyloid-beta peptide, *Faseb J.* 18 (2004) 836–838.
- [68] S. Subasinghe, S. Unabia, C.J. Barrow, S.S. Mok, M.I. Aguilar, D.H. Small, Cholesterol is necessary both for the toxic effect of Abeta peptides on vascular smooth muscle cells and for Abeta binding to vascular smooth muscle cell membranes, *J. Neurochem.* 84 (2003) 471–479.
- [69] S.S. Wang, D.L. Rymer, T.A. Good, Reduction in cholesterol and sialic acid content protects cells from the toxic effects of beta-amyloid peptides, *J. Biol. Chem.* 276 (2001) 42027–42034.
- [70] S. Oddo, A. Caccamo, I.F. Smith, K.N. Green, F.M. LaFerla, A dynamic relationship between intracellular and extracellular pools of Abeta, *Am. J. Pathol.* 168 (2006) 184–194.